Journal of Hazard Literacy
eISSN 3091-6402

Review Article
J. Hazard Lit. 2026;2(1):e19
https://doi.org/10.63737/jhl.25.0041

Geochemical responses of groundwater to earthquakes: a review

Hyejung Jung, Jeonghoon Lee*
Department of Science Education (Earth Sciences), Ewha Womans University, Seoul, Korea

Abstract

Earthquakes, as major natural hazards, generate substantial disturbances within the subsurface that alter the hydraulic and structural properties of geological formations and trigger diverse hydrogeochemical responses in groundwater systems. In addition to hydrological effects such as groundwater-level fluctuations, seismic events are known to induce anomalies in groundwater chemistry, dissolved gases (He, Rn, CO_2, CH_4, and H_2), stable and radiogenic isotopes ($\delta^{13}C$–DIC, $\delta^{18}O$, $\delta^{2}H$, $\delta^{34}S$, $^{87}Sr/^{86}Sr$, and $^{3}He/^{4}He$), and redox-sensitive and microbially-mediated species. These perturbations reflect processes including micro-fracturing, permeability enhancement, fluid–rock interaction, deep-fluid migration, and biogeochemical activation. Despite growing interest in their potential to illuminate subsurface dynamic processes, the interpretation of earthquake-related hydrogeochemical anomalies remains challenging due to strong geological variability, non-seismic forcing factors, and limitations in long-term monitoring. This review synthesizes current understanding of hydrogeochemical responses to earthquakes, evaluates mechanistic linkages supported by case studies, and discusses future directions for improving interpretation of transient geochemical signals and their broader implications within seismic hazard science.

Keywords: natural disasters, earthquakes, groundwater, isotopes, water-rock interactions

Received: Nov 25, 2025
Revised: Dec 28, 2025
Accepted: Jan 26, 2026

***Corresponding author**
Jeonghoon Lee
Department of Science Education (Earth Sciences), Ewha Womans University, Seoul, Korea
Tel: +82-2-3277-3794
E-mail: jeonghoon.d.lee@gmail.com

ORCID
Hyejung Jung
https://orcid.org/0000-0003-0211-6501
Jeonghoon Lee
https://orcid.org/0000-0002-1256-4431

Conflict of interest
No potential conflict of interest relevant to this article was reported.

Funding sources
This work was supported by the Ministry of Education of the Republic of Korea and the National Research Foundation of Korea (NRF-2024S1A5C3A03046593).

Acknowledgements
Not applicable.

Introduction

Earthquakes generate widespread physical disruption within the subsurface, altering the structural and hydraulic properties of geological materials and influencing groundwater systems [1]. While numerous studies have examined hydrological responses such as groundwater-level changes, pore-pressure fluctuations, and liquefaction, recent research has increasingly focused on hydrogeochemical signatures generated by seismic events and their potential to illuminate subsurface processes [2]. Observed geochemical anomalies include changes in major and trace ion chemistry, dissolved gas concentrations (He, Rn, CO_2, CH_4, and H_2), isotopic compositions ($\delta^{13}C$–DIC, $\delta^{18}O$, $\delta^{2}H$, and $^{3}He/^{4}He$), and redox-sensitive compounds, often recorded before, during, or after major earthquakes [3–5]. These variations reflect dynamic interactions among mechanical rock deformation, enhanced permeability, fluid–rock interaction, and deep fluid migration stimulated by seismic activity (Fig. 1) [6,7].

Recent progress in high-frequency monitoring and analytical instrumentation has increased the ability to detect subtle hydrogeochemical signals associated with crustal deformation. Continuous multi-parameter groundwater observatories have revealed transient anomalies in radon, helium,

Availability of data and material
Upon reasonable request, the datasets of this study can be available from the corresponding author.

Authors' contributions
Conceptualization: Jung H, Lee J.
Methodology: Jung H, Lee J.
Investigation: Jung H.
Writing - original draft: Jung H.
Writing - review & editing: Jung H, Lee J.

Ethics approval and consent to participate
Not applicable.

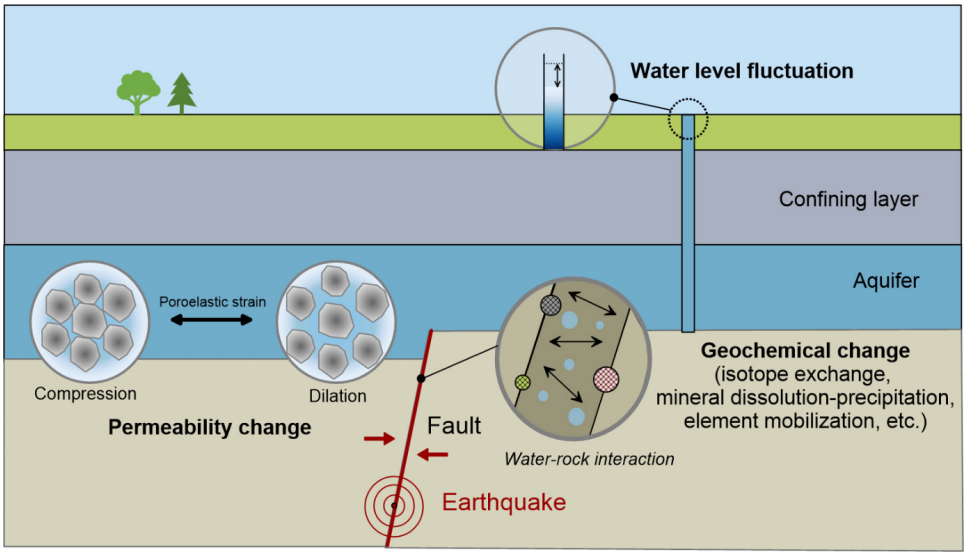

Fig. 1. Conceptual model of earthquake-driven hydrogeochemical processes. Seismic slip along a fault generates poroelastic strain that alternates between compression and dilation, modifying permeability in the surrounding aquifer and fault damage zone. The resulting fluid redistribution facilitates water–rock interaction and induces geochemical changes, including isotope exchange and mineral dissolution–precipitation, which can mobilize solutes and alter groundwater chemistry. These subsurface responses may propagate to the surface and manifest as well water level fluctuations.

hydrogen, major ions, and isotopes that are difficult to attribute to hydrological or climatic drivers alone [8,9]. These technological advances, combined with increasing evidence of chemical precursors prior to seismic rupture, have stimulated growing interest in the potential use of hydrogeochemical indicators for understanding subsurface processes and for contributing to multi-parameter seismic monitoring frameworks [10,11].

Understanding the generation mechanisms and temporal characteristics of earthquake-related geochemical signals is critical because such anomalies can serve as valuable indicators of subsurface change. These signals may also have broader implications for groundwater resource security, environmental risk evaluation, and crustal fluid circulation [12,13]. Although promising evidence supports the hypothesis that hydrogeochemical signals may act as precursors or early indicators of seismic processes, significant uncertainties remain. These uncertainties arise from variability among geological settings, monitoring limitations, and interference from non-seismic forcing factors such as seasonal recharge or anthropogenic disturbances [4,14]. This review synthesizes current knowledge on earthquake-induced geochemical responses within groundwater systems, with a focus on elucidating the mechanistic coupling between seismic deformation, permeability changes, fluid migration, and geochemical reactivity. We identify and evaluate the processes responsible for generating chemical and isotopic anomalies, compare observational case studies from major earthquakes globally, and assess advances in monitoring and analytical technologies that enable detection of transient hydrogeochemical signals. By establishing a unified conceptual framework and highlighting critical knowledge gaps, this review provides direction for future research aimed at improving the interpretation and practical application of hydrogeochemical indicators in understanding subsurface responses to earthquakes.

Physical Processes Enabling Geochemical Changes During Earthquakes

Earthquakes induce a broad range of physical disturbances within the crust that modify subsurface hydraulic and structural conditions, thereby enabling geochemical and isotopic anomalies to develop in groundwater. Seismic stress perturbations cause deformation of rock matrices through micro-fracturing, dilation of pre-existing faults, and reactivation of fracture networks, fundamentally reshaping pore geometry and interconnected flow pathways [15,16]. The creation of new reactive mineral surfaces enhances water–rock interaction kinetics, accelerating mineral dissolution and isotopic exchange that contribute to detectable chemical variation following seismic events [17].

Simultaneously, earthquakes produce transient increases in aquifer permeability through fracture opening, unclogging of mineral precipitates, and mobilization of fine sediments, which promote temporary or persistent changes in hydraulic connectivity between previously isolated reservoirs [1,7,18]. These structural adjustments generate hydrological responses including rapid fluctuations in groundwater level, oscillations in pore pressure, and changes in spring discharge that occur within seconds to days after seismic shaking [19,20]. Groundwater-level rises are commonly associated with pore-pressure increases arising from compaction or liquefaction, or with fracture closure that reduces aquifer storage volume, whereas declines typically result from fracture opening and increased drainage capacity that facilitate downward or lateral flow [1,18]. This conceptual relationship between stress-induced structural adjustments and groundwater-level change is summarized in Fig. 2. Such hydraulic responses form a critical physical context for interpreting subsequent chemical and isotopic changes.

Permeability enhancement and fluid-pathway rearrangement create conduits through which deep crustal or hydrothermal fluids rich in dissolved gases such as He, Rn, CO_2, CH_4, and H_2 can ascend and mix with shallow groundwater, producing abrupt shifts in ionic composition, silica concentration, carbonate equilibria, and isotopic ratios [3,4,10]. Noble-gas anomalies, particularly elevated $^3He/^4He$ ratios, are widely interpreted as indicators of mantle or deep-crustal input activated by rupture propagation [3]. Rapid fluctuations in pressure and temperature also influence mineral solubility, degassing dynamics, and redox stability, mobilizing geochemical

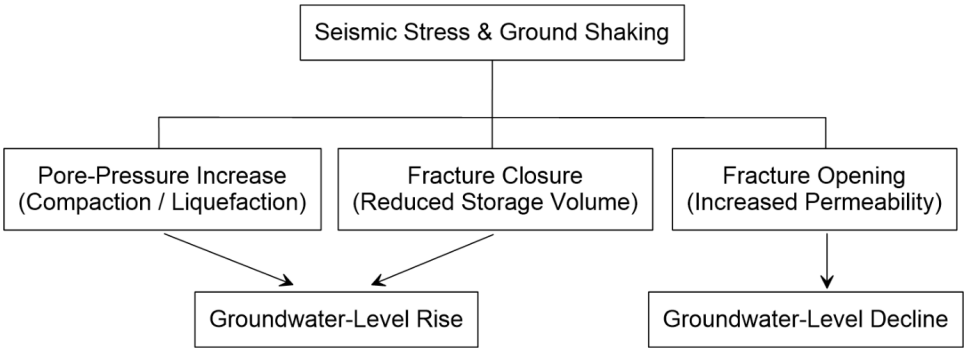

Fig. 2. Conceptual schematic illustrating groundwater-level responses to earthquakes. Earthquake-induced seismic stress and ground shaking can trigger contrasting groundwater-level changes depending on subsurface structural and hydraulic conditions. Increased pore pressure, liquefaction, and fracture closure may generate rapid groundwater-level rises, whereas permeability enhancement, fracture opening, and increased drainage can lead to groundwater-level decline. The direction and magnitude of groundwater-level responses vary with fault-zone architecture, aquifer properties, and stress state, and may occur either co-seismically or persist for days to months following a seismic event.

species including Fe-Mn oxyhydroxides, sulfate, and carbonate minerals [21,22]. Pressure release accompanying fracture dilation can further promote degassing and supersaturation, reshaping the chemical speciation of carbon and silica.

In addition to purely physical mixing, the redistribution of electron donors and acceptors along newly established flow paths can stimulate microbial metabolic activity, facilitating redox transitions and promoting the biogenic production or consumption of dissolved constituents such as methane, ammonium, nitrate, and sulfate [23,24]. Co-seismic increases in CH_4, Fe^{2+}, and Mn^{2+} and decreases in sulfate have been interpreted as evidence for microbially-mediated transformations superimposed on physical flow-driven processes [10]. These observations highlight that earthquake-triggered hydrogeochemical anomalies reflect the coupled behavior of mechanical deformation, hydrological perturbation, geochemical reactions, and biological activity [25].

Together, these interconnected physical processes form the mechanistic foundation supporting observable hydrogeochemical responses to earthquakes, including variations in major and trace ions, dissolved gases, isotopic compositions, and redox-sensitive species. Understanding the physical drivers of permeability restructuring, groundwater-level dynamics, and pressure-flow redistribution is therefore essential for interpreting the geochemical anomaly patterns examined in the following section.

Types of Hydrogeochemical Responses to Seismic Events

Earthquakes trigger diverse hydrogeochemical anomalies within groundwater systems, reflecting the coupling between crustal deformation, permeability enhancement, fluid mobilization, redox restructuring, and microbial activation. These chemical and isotopic responses, including variations in major and trace ions, dissolved gas concentrations, stable and radiogenic isotope compositions, and redox-sensitive species and microbial activity, serve as indicators of subsurface stress redistribution and fluid–rock interaction processes (Table 1) [2,7].

Major ions such as Ca^{2+}, Mg^{2+}, Na^{+}, K^{+}, HCO_3^{-}, SO_4^{2-}, Cl^{-}, NO_3^{-} and SiO_2 frequently display rapid increases or decreases following seismic perturbations, reflecting accelerated mineral dissolution, mobilization of solute-rich pore fluids, and mixing between deep and shallow groundwater reservoirs [1,26–28]. Mobilization peaks in trace elements including Fe, Mn, As,

Table 1. Hydrochemical indicator matrix: key parameters responsive to earthquake-induced subsurface changes

Indicator category	Specific parameters	Typical response to seismic forcing	Interpretation / mechanistic link	Representative references
Major ions	Ca^{2+}, Mg^{2+}, Na^{+}, K^{+}, HCO_3^{-}, SO_4^{2-}, Cl^{-}, SiO_2	Sudden increases or decreases; directional shifts pre-/post-event	Enhanced dissolution/precipitation, mixing of deep vs shallow fluids, change in flow path	[44, 49, 51, 53, 54]
Trace metals / elements	Fe, Mn, As, Li, Sr, REE	Mobilization peaks, enrichment factors increase	Redox shifts, rock-water interaction, deep fluid input	[44, 52, 53]
Dissolved gases	He, Rn (^{222}Rn, ^{220}Rn), CO_2, CH_4, H_2	Sharp spikes, anomalous timing ahead/after quake	Fracture opening, deep fluid release, gas exsolution	[50, 58–60]
Stable / radio isotopes	$\delta^{13}C$-DIC, $\delta^{18}O$, $\delta^{2}H$, $^{3}He/^{4}He$, $^{87}Sr/^{86}Sr$	Isotopic shifts, mixing trends, signature changes	Source mixing, fluid–rock reaction, mantle or crust fluid input	[47, 49, 52, 57, 61]
Hydraulic / physical proxy indicators	Groundwater level, pore-pressure, temperature, EC, Total dissolved solids (TDS)	Co-seismic jumps, transient anomalies	Changes in hydraulic connectivity, enhanced permeability	[45, 48, 54, 60]

EC, electrical conductivity.

Li, and Sr have similarly been reported after major earthquakes and interpreted as signatures of redox restructuring and enhanced interaction between circulating groundwater and reactive mineral phases [4,29]. Notably, Barberio et al. [30] observed that concentrations of As, V, and Fe increased several months prior to the 2016 Amatrice-Norcia earthquake, suggesting that progressive crustal dilation and permeability enhancement can mobilize trace metals before fault failure, whereas Cr exhibited a sharp post-seismic increase associated with fracture flushing and sudden pathway opening. Such chemical responses are commonly linked to transient permeability enhancement and restructuring of flow paths that transport stored fluids from previously isolated pore domains through fracture dilation and permeability reorganization (Fig. 3) [19].

Dissolved gas anomalies represent some of the most sensitive hydrogeochemical indicators of seismic strain. Sharp increases in He, Rn, CO_2, CH_4, and H_2 concentrations have been widely documented before or after earthquakes, particularly in wells proximal to active fault structures [25,31]. Radon (^{222}Rn), although transported as a dissolved gas, functions as a radiogenic tracer whose short half-life and decay-derived production make it particularly responsive to fracture propagation, stress accumulation, and transient enhancement of permeability [32–35]. Noble-gas ratios such as elevated $^{3}He/^{4}He$ provide direct evidence for the ascent of deep crustal or mantle-derived fluids through newly opened or unclogged fractures [3,36]. Together, these gas tracers offer powerful diagnostic tools for identifying fluid-source contributions and permeability evolution during seismic cycles.

Stable and radiogenic isotopes including $\delta^{13}C$–DIC, $\delta^{18}O$, $\delta^{2}H$, $\delta^{34}S$, and $^{87}Sr/^{86}Sr$ provide complementary insights into water–rock interactions, degassing, redox transformations, and mixing processes that are activated or reorganized by seismic deformation [10,37]. Transient enrichment of $\delta^{18}O$ in groundwater following seismic events has been attributed to fracture-induced increases in reactive surface area that facilitate oxygen isotope exchange between water and mineral lattices, particularly carbonates and silicates, under conditions of enhanced flow and pressure change [3,38]. In many cases, the combination of longer contact time along newly opened fracture surfaces and increased CO_2 partial pressure promotes carbonate dissolution and re-precipitation, which further drives $\delta^{18}O$ of the aqueous phase away from its original meteoric composition toward rock-buffered values. Where $\delta^{2}H$ remains nearly constant while $\delta^{18}O$ increases, such patterns are consistent with water–rock isotope exchange rather than evaporation or simple meteoric mixing (Fig. 4). Fig. 4 illustrates a $\delta^{18}O$ only shift following earthquake-

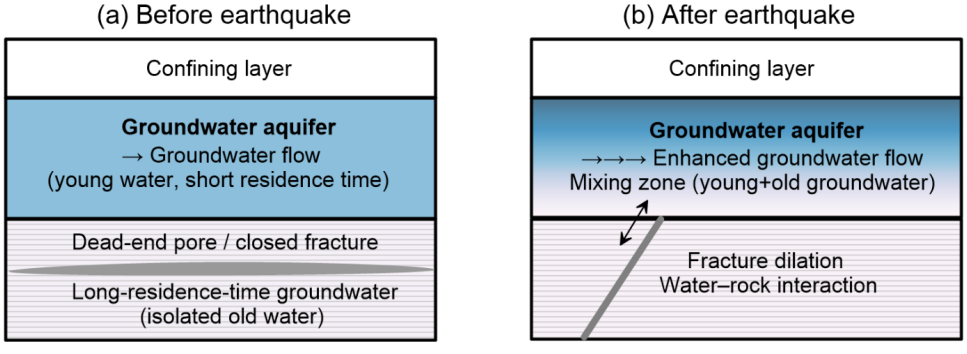

Fig. 3. Conceptual illustration of hydrogeological and geochemical responses to earthquakes. Prior to seismic activity, sealed fractures restrict flow pathways and isolate long-residence-time groundwater. Seismic slip induces fracture dilation and permeability enhancement, accelerating groundwater flow and generating a mixing zone between young and old groundwater. These hydraulic changes enable enhanced water–rock interaction that may produce measurable hydrogeochemical anomalies. Modified from Lee et al. [56].

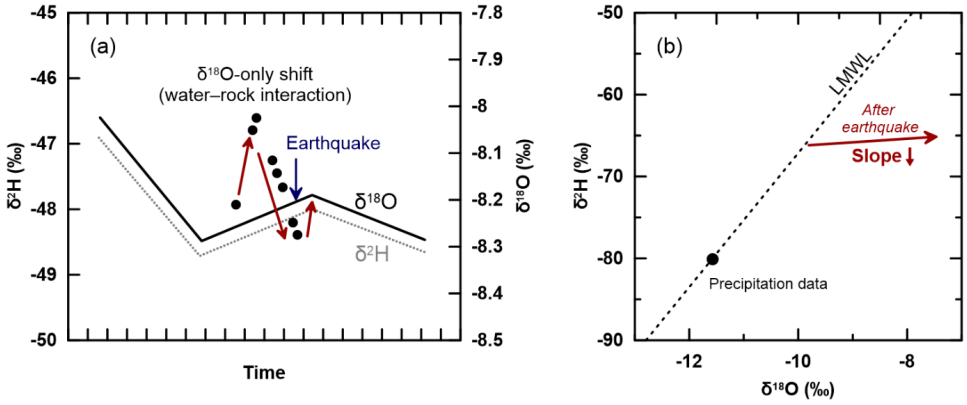

Fig. 4. Conceptual representation of isotope responses to earthquakes. (a) Temporal changes in $\delta^{18}O$ and $\delta^{2}H$ of groundwater. The solid black lines represent the background seasonal isotope trend observed under non-seismic conditions. Black circles represent individual $\delta^{18}O$ values of groundwater samples measured from the pre-seismic to post-seismic period, showing deviations from the background seasonal trend. These data illustrate a progressive $\delta^{18}O$ enrichment that begins prior to the earthquake and continues afterward, interpreted as water–rock oxygen isotope exchange triggered by seismic microfracturing, whereas $\delta^{2}H$ shows negligible variation, excluding evaporation or meteoric dilution. (b) $\delta^{2}H$–$\delta^{18}O$ relationship showing a post-earthquake decrease in isotopic slope relative to the local meteoric water line (LMWL), reflecting $\delta^{18}O$-only enrichment rather than a coupled $\delta^{18}O$–$\delta^{2}H$ trend expected for evaporative processes. Red arrows indicate the direction of post-seismic isotopic evolution.

induced microfracturing and a corresponding post-seismic decrease in the $\delta^{2}H$–$\delta^{18}O$ slope relative to the local meteoric water line (LMWL), distinguishing selective isotope exchange from evaporative fractionation.

$\delta^{13}C$–DIC reflect changes in the balance among deep CO_2 input, carbonate dissolution and precipitation, and microbially mediated carbon cycling [39,40]. During crustal deformation and fault rupture, increases in permeability and frictional heating can promote the release of deeply sourced CO_2 originating from mantle and marine carbonate reservoirs, which inherently possess relatively heavy $\delta^{13}C$ signatures (0‰ to −4‰) compared to microbially derived or soil-respired CO_2 (−26‰ to −12‰). In addition, dissolution of this deep CO_2 into formation waters further enriches $\delta^{13}C$–DIC due to positive isotope fractionation during CO_2– HCO_3^- conversion, driving DIC values upward by an additional +7‰ to +9‰. Liang et al. [39] documented a pronounced pre-seismic increase in $\delta^{13}C$ (CO_2–DIC) in hot springs associated with thermal decomposition of carbonate minerals caused by fault frictional heating, followed by a sharp post-seismic decline as pressure dropped and CO_2 degassing intensified. Similarly, Liu et al. [40] reported broad spatial variability in $\delta^{13}C$-DIC (−11.6‰ to 0.1‰) across the Maduo rupture zone, where positive excursions corresponded to enhanced contributions from deep CO_2 within widened fault pathways, while negative shifts reflected increased fluxes of shallow organic-carbon-rich waters under newly reducing post-seismic conditions. These contrasting pathways demonstrate that $\delta^{13}C$–DIC is a sensitive tracer of fault-controlled carbon mobilization during seismic cycles, enabling differentiation between deep CO_2 degassing, carbonate buffering, and microbially-mediated carbon transformations.

Sulfur isotope variations ($\delta^{34}S$) provide valuable constraints on the sources and transformation pathways of sulfur within fault-controlled hydrothermal systems. Following the 2016 Kumamoto earthquake, seismic enhancement of permeability allowed deep hydrothermal fluids enriched in sulfate to ascend to the surface through newly formed fracture networks, producing unusually high $\delta^{34}S$–SO_4^{2-} values in newly appeared saline springs. Hosono et al. [41] interpreted these elevated $\delta^{34}S$ signatures as evidence for sulfur derived from magmatic SO_2 disproportionation or from microbial sulfate reduction under reducing deep aquifer conditions, both of which

preferentially enrich the remaining dissolved sulfate in $\delta^{34}S$. Thus, $\delta^{34}S$ shifts serve as indicators of seismically driven fluid mobilization and evolving redox conditions in volcanic hydrothermal environments.

Earthquake perturbations can modify groundwater pathways and consequently alter the extent of water–rock interaction and lithologic mixing, which is recorded in changes in Sr isotopic composition ($^{87}Sr/^{86}Sr$) [42,43]. Wang et al. [42] demonstrated that $^{87}Sr/^{86}Sr$ ratios of Fujian thermal springs range from approximately 0.706 to 0.726, with higher values linked to aluminosilicate weathering sources (0.716–0.720) and lower values to carbonate–sulfate sources (~0.708), indicating that Sr isotopic composition is strongly controlled by lithology and the degree of water–rock interaction. Kim et al. [43] found that groundwater $^{87}Sr/^{86}Sr$ ratios in the Gyeongju earthquake area ranged from 0.705688 to 0.712368 and varied systematically with bedrock type, with more radiogenic values observed in granite-dominated fractured aquifers due to interaction with Rb/Sr-rich minerals such as feldspar and biotite.

Finally, hydraulic indicators such as groundwater-level fluctuations, pore-pressure anomalies, electrical conductivity (EC), temperature, and total dissolved solids (TDS) provide essential contextual proxies for interpreting the origin and timing of hydrogeochemical anomalies [1,2,18].

Observational Evidence from Case Studies

A wide array of field investigations across diverse tectonic settings has documented hydrogeochemical responses of groundwater to seismic events (Table 2). These case studies illustrate the variability in chemical signals generated during earthquakes and highlight the importance of geological context, aquifer structure, and monitoring resolution in interpreting geochemical anomalies.

The earthquakes discussed in Sections 4.1–4.5 were selected based on three criteria: (1) the availability of high-resolution, multi-parameter groundwater datasets (groundwater level, hydrochemistry, isotopes, and/or gas tracers); (2) well-documented pre-, co-, and post-seismic hydrogeochemical responses; and (3) coverage of diverse tectonic and hydrogeological settings, including plate-boundary earthquakes (Chi-Chi, Wenchuan, Kumamoto, Japan), intraplate seismicity (Gyeongju, Korea), and induced seismicity associated with enhanced geothermal systems (EGS; Pohang, Korea). Together, these case studies provide a representative framework for evaluating how different seismic sources and geological contexts control groundwater responses to earthquakes.

Chi-Chi earthquake (1999, Taiwan)

The 1999 Mw 7.6 Chi-Chi earthquake in Taiwan reorganized groundwater flow, induced transient pore-pressure redistribution, and alter hydrochemical and isotopic characteristics within fault-controlled aquifer systems. Hydrogeochemical observations show diverse pre-, co-, and post-seismic responses across multiple aquifer settings, with implications for crustal fluid dynamics and earthquake precursors. Long-term analysis of commercially bottled groundwater documented substantial increases in SO_4^{2-} and NO_3^- within months preceding the mainshock. These concentrations then decreased rapidly shortly before rupture, suggesting stress-induced hydrological redistribution and enhanced mixing between deep and shallow groundwater [44].

Regional monitoring revealed four distinct types of groundwater-level responses, ranging from abrupt co-seismic rises to sustained declines or step-like recovery patterns. These patterns

Table 2. Representative earthquake events and associated hydrogeochemical responses observed in groundwater systems

Earthquake case	Region / Mw	Dominant hydrogeochemical responses	Interpretation / mechanisms	Monitoring type	Key references
Chi-Chi 1999	Taiwan / Mw 7.6	- Groundwater level changes - SO_4^{2-} & NO_3^- chemical anomalies - $\delta^{18}O$ shift (river–aquifer mixing)	- Pore-pressure redistribution - Fault-zone permeability enhancement - Deep–shallow water mixing - Pre-seismic aquifer disturbance	- Regional well network - Long-term groundwater chemistry - Time-series & spectral analysis	[44–48]
Wenchuan 2008	China / Mw 7.9	- Large increases in K^+, SO_4^{2-}, TDS - $\delta^{18}O$–δ^2H anomalies - Strong increase in $^3He/^4He$ & CO_2 gas	- Deep-fluid influx & mantle-derived gases - Water-rock interaction enhancement - Flow-path reorganization along active faults	- Hot spring monitoring campaign - Gas & isotope sampling at multiple spring sites	[49–51]
Tohoku 2011	Japan / Mw 9.0	- Co-seismic groundwater-level changes - Radon anomalies in groundwater - Increased $^3He/^4He$ ratios in hot springs - Temperature & discharge anomalies	- Elastic strain & pore-pressure redistribution - Fracture dilation & permeability enhancement - Deep-fluid upwelling & mantle helium input - Strain-controlled degassing processes	- Continuous groundwater-level monitoring - Hydrochemistry & radon records - Noble gas isotopes - Multi-year datasets	[59–61]
Kumamoto 2016	Japan / Mw 7.0	- Co-seismic groundwater level decrease followed by post-seismic recovery - δ^2H–$\delta^{18}O$ values shifted toward mountain-derived meteoric water - Appearance of newly formed saline springs - Increased concentrations of SO_4^{2-}, Li, and B - Enrichment of $\delta^{34}S$–SO_4^{2-} - Decrease in $^3He/^4He$ ratio	- Permeability enhancement and fracture dilation - Release of mountain aquifer water into lower elevations - Upwelling of deep hydrothermal fluids - Strain-controlled degassing processes - Progressive crustal strain accumulation reflected in aquifer system	- Continuous groundwater-level observations - Long-term hydrochemical time series - Stable isotopes and noble gas isotope measurements - Multi-year monitoring network	[3,20,41,52]
Tottori 2016	Japan / Mw 6.6	- $\delta^{18}O$ anomaly in groundwater	- Enhanced water-rock interaction via micro-fracturing and newly exposed surfaces	- Groundwater monitoring well	[38]
Gyeongju 2016	South Korea / Mw 5.4–5.5	- Groundwater-level anomalies in confined aquifers - $\delta^{18}O$–δ^2H & $\delta^{13}C$ changes - Elevated ^{222}Rn	- Confined-aquifer hydraulic response - Deep fluid mixing & fracture activation - Local fault-controlled flow	- Continuous groundwater monitoring network - Hydrochemistry time-series analysis	[26, 43, 53, 55]
Pohang 2017	South Korea / Mw 5.4	- Sharp groundwater-level decrease (EGS boreholes) - $\delta^{18}O$-δ^2H, $^{87}Sr/^{86}Sr$, ^{222}Rn anomalies - Thoron (^{220}Rn) and microbial shifts	- Deep formation-water discharge - Hydraulic stimulation induced permeability change - Rapid water–rock interaction & saline fluid influx	- Groundwater monitoring well - Gas & isotope monitoring	[54, 57, 62]

indicate that pore-pressure redistribution, rather than permanent permeability change, dominated the regional post-seismic hydrological adjustment [45]. Time-series decomposition and spectral analyses identified anomalous groundwater-level fluctuations in confined aquifers during the weeks preceding the earthquake. These results suggest that frequency-domain analysis can detect subtle pre-seismic hydrological anomalies not visible in raw time-series records [46].

Stable isotope monitoring further illustrated substantial post-seismic changes in $\delta^{18}O$, indicating enhanced river–aquifer interaction and increased cross-aquifer exchange due to the fracturing of confining units and the establishment of new hydraulic links following the rupture [47]. The magnitude, polarity, and persistence of earthquake-induced groundwater-level responses depend primarily on hydrogeological characteristics such as confinement, compressibility, and permeability contrasts rather than earthquake magnitude alone. Confined

aquifers exhibit prolonged step-type shifts, whereas unconfined aquifers show transient oscillatory behavior [48].

Together, these studies provide a coherent framework for understanding how large earthquakes perturb groundwater systems through dynamic strain, co-seismic pore-pressure redistribution, and post-seismic flow-path reorganization. The Chi-Chi earthquake record highlights the diagnostic potential of integrated hydrochemical, isotopic, and groundwater-level monitoring for assessing crustal permeability evolution and for identifying hydrological indicators relevant to earthquake forecasting and fault-zone fluid processes.

Wenchuan earthquake (2008, China)

Hydrogeochemical and gas-geochemical observations following the Wenchuan earthquake (Mw 7.9; MS 8.0) revealed pronounced anomalies in hot spring chemistry and gas compositions, including elevated $^{3}He/^{4}He$ ratios and CO_2 concentrations near major active fault zones. These anomalies indicate enhanced permeability and deep-fluid migration driven by co-seismic crustal deformation [49,50]. The 2008 Wenchuan earthquake in western Sichuan is a representative example that illustrates large-scale fluid mobilization in active tectonic regions. K^+ and SO_4^{2-} concentrations increased and $\delta^{18}O$ and $\delta^{2}H$ values in hot spring waters shifted before and after the earthquake. These changes were interpreted as evidence of enhanced contributions from deep hydrothermal fluids and intensified water–rock interactions [49]. Gas-geochemical observations showed substantial increases in $^{3}He/^{4}He$ and $\delta^{13}C–CO_2$ in hot spring discharges along the Longmenshan and Xianshuihe fault belts, indicating the upward migration of mantle-derived fluids facilitated by increased crustal permeability after the earthquake [50]. Over time, mantle signals decreased while crustal CH_4 and radiogenic helium increased, reflecting progressive re-equilibration of the aquifer and hydrothermal system.

The role of seismically induced permeability enhancement and CO_2-driven carbonate dissolution was further supported by observations from the 2013 Lushan MS 7.0 earthquake in the same tectonic setting [51]. Shortly after the mainshock, hot springs in the Kangding district exhibited substantial increases in Ca^{2+}, HCO_3^-, and TDS concentrations within three to five days, interpreted as the result of accelerated dissolution of carbonate rocks and the inflow of deep groundwater. In contrast, decreases in Na^+, Cl^-, and SO_4^{2-} recorded at other sites indicate dilution by shallow meteoric waters [51]. Shifts in hydrochemical facies confirmed active mixing of fluids from different depths as pore pressures and flow pathways adjusted during the aftershock period.

Together, these studies demonstrate that large and moderate earthquakes can fundamentally alter fluid circulation within fault zones through permeability perturbation, deep fluid ascent, water–rock reaction intensification, and mixing processes. Hydrochemical and gas-geochemical indicators such as Ca^{2+}, HCO_3^-, K^+, SO_4^{2-}, TDS, $^{3}He/^{4}He$, and CO_2 provide sensitive records of post-seismic hydrological restructuring and serve as important tools for understanding earthquake-related crustal fluid dynamics.

Kumamoto earthquake (2016, Japan)

The 2016 Mw 7.0 Kumamoto earthquake provides a comprehensive observational datasets to date for understanding hydrogeochemical responses to seismic deformation. Multiple independent studies have documented rapid and persistent changes in groundwater levels, solute chemistry, and isotopic tracers following major earthquakes. These observations demonstrate that earthquake-induced permeability enhancement reorganizes groundwater flow systems across regional scales. Immediately after the mainshock, groundwater levels in confined

aquifers along the Futagawa–Hinagu fault zone exhibited a sharp co-seismic decline of up to approximately 4.7 m within the first 30–45 days, driven by rapid drainage through newly dilated fracture networks [52]. This drawdown was followed by a delayed but substantial post-seismic rise in groundwater levels, reaching increases of nearly 11 m over the following months. Permeability enhancement enabled the release of stored groundwater from mountain aquifers and its downslope transport, a process supported by the post-seismic convergence of $\delta^{2}H$–$\delta^{18}O$ values toward those of mountain spring waters [52].

Geochemical evidence further supports the mobilization of deep fluids during and after the earthquake. Newly formed saline springs emerging after the mainshock displayed elevated concentrations of SO_4^{2-}, Li, and B, as well as unusually high $\delta^{34}S$–SO_4^{2-} values (10.5‰–17.5‰), indicating upwelling of hydrothermal fluids through seismically activated fracture conduits [41]. Noble-gas observations similarly reveal strong coupling between mechanical strain and subsurface fluid behavior: $^{3}He/^{4}He$ ratios in deep groundwater declined significantly following the earthquake, with spatial and temporal variations correlating closely with modeled volumetric strain, implying microfracturing-induced release of radiogenic ^{4}He from the crust [3]. Long-term groundwater level analysis also identified multi-year precursory deviations beginning around 2014, during which levels remained consistently below modeled predictions before recovering toward the time of rupture; these patterns parallel global navigation satellite system-derived strain accumulation and highlight the capacity of volcanic aquifers to record pre-seismic deformation [20].

These datasets define a coherent sequence of hydrological and geochemical responses to the Kumamoto earthquake: (1) co-seismic drawdown due to fracture dilation, (2) delayed post-seismic recharge driven by permeability enhancement, (3) mobilization of deep solute-rich fluids, (4) strain-controlled noble-gas anomalies, and (5) multi-year hydrologic precursors reflecting progressive crustal strain buildup. The Kumamoto case thus represents a uniquely well-documented natural laboratory demonstrating how seismic deformation reorganizes groundwater flow and alters hydrogeochemical signatures, providing crucial guidance for developing multi-parameter monitoring frameworks to evaluate evolving crustal conditions.

Gyeongju earthquake (2016, South Korea)

The 2016 Mw 5.4–5.5 Gyeongju earthquake affected groundwater hydrology and geochemistry within the Yangsan Fault System. A series of investigations demonstrated diverse co- and post-seismic responses dependent on aquifer type, lithology, and fault-zone hydraulic properties. Groundwater-level changes were predominantly observed in confined fractured bedrock aquifers, while shallow alluvial aquifers exhibited minimal response. These patterns indicate that permeability enhancement and pressure redistribution primarily affected deeper, fault-connected flow systems [53]. $^{3}He/^{4}He$, ^{222}Rn, $\delta^{18}O$, $\delta^{2}H$, and $\delta^{13}C$ signatures indicate upwelling of older, deeper groundwater following the earthquake based on depleted stable isotopes and low tritium concentrations. These results support post-seismic deep-fluid intrusion associated with seismic fracture opening. Elevated ^{222}Rn and $\delta^{13}C$ anomalies were most pronounced near the epicenter, demonstrating the influence of bedrock lithology and fault orientation on fluid migration pathways [54].

Hydrochemical studies integrating groundwater-level, temperature, EC, radon, and strontium isotope measurements identified distinct post-seismic behaviors among groups of wells, interpreted using self-organizing map (SOM) clustering. The hydrogeological responses were classified into mechanisms including (1) water–rock interaction and dissolution mobilization, (2) mixing between shallow and deep aquifers, (3) fracture network activation related to strike-

slip movement, and (4) no response in hydraulically isolated systems [43]. Additional time-series analysis showed that groundwater-level shifts could be characterized into transient, step-like, and persistent response types, with confined wells along fault boundaries displaying the strongest anomalies, suggesting dynamic stress effects controlling fracture permeability and pore-pressure propagation [55]. Seismic-induced changes strongly depend on confinement conditions and screened interval design, reinforcing the importance of hydrogeological characterization for effective interpretation of seismic-hydrological monitoring [56].

These studies confirm that the Gyeongju earthquake reorganized groundwater flow pathways through permeability enhancement, deep fluid ascent, and pressure redistribution. Integrated hydrochemical and isotopic monitoring provides essential tools for interpreting fracture network dynamics and evaluating the hydromechanical feedback between faulting and groundwater circulation in intraplate seismic regions.

Pohang earthquake (2017, South Korea)

The 2017 Mw 5.5 Pohang earthquake in Korea represents a key example illustrating how induced seismicity associated with EGS stimulation can substantially perturb groundwater flow dynamics and hydrogeochemical conditions within fractured basement rock environments. Co- and post-seismic anomalies in groundwater level, hydrochemistry, isotopes, and noble gases around the Pohang EGS site reflect reorganization of subsurface flow paths and mobilization of deep fluids. Continuous hydrogeochemical monitoring across regional observation wells documented abrupt changes in groundwater level and marked fluctuations in EC, temperature, $\delta^{18}O$, $\delta^{2}H$, $^{87}Sr/^{86}Sr$, and ^{222}Rn following the earthquake. These changes provide evidence for co-seismic permeability enhancement, deep fluid upwelling, and rapid water–rock interactions not explainable by poroelastic mechanisms alone [54]. Well flow responses recorded from the EGS boreholes demonstrated that both moderate induced events (Mw 3.2) and the mainshock triggered rapid discharge of deep formation water, accompanied by significant isotopic deviations from the LMWL and sharp declines in hydraulic head. These responses indicate pressure-driven expulsion of deeply circulated fluids along critically stressed fault zones [57]. Chemical and isotopic signatures revealed saline and thermally altered fluid components derived from several kilometers depth. These results support feedback coupling between fault rupture and high-pressure fluid migration during stimulation operations. More recent research further showed that thoron (^{220}Rn) anomalies and changes in microbial community structure serve as highly sensitive tracers of active fracture zones and short-lived permeability enhancements. These indicators demonstrate strong diagnostic potential for monitoring real-time seismic responses in groundwater systems [58].

These studies indicate that the Pohang event fundamentally reorganized subsurface hydraulic pathways through fault reactivation and deep-fluid mobilization. Groundwater-based indicators including stable isotopes, Sr isotopes, radon, and microbial fingerprints offer powerful tools for characterizing induced seismic processes and for improving assessments of hydromechanical coupling in fractured rock geothermal environments.

Monitoring and Analytical Approaches

Integrated hydrogeological, hydrochemical, isotopic, and gas-geochemical monitoring approaches have proven essential for understanding earthquake-induced perturbations in groundwater systems and for differentiating elastic pore-pressure responses from deep-fluid

mobilization processes. Continuous groundwater-level and physicochemical monitoring (including temperature and EC) using high-frequency digital loggers has enabled detailed characterization of abrupt co-seismic steps, delayed recovery patterns, and transient oscillatory fluctuations associated with dynamic strain. Such datasets have been used to classify groundwater responses into distinct hydrological types and to evaluate the roles of aquifer confinement, lithology, and fault connectivity in controlling hydraulic behavior following seismic events [26,45,48].

Environmental tracers such as $\delta^{18}O$, $\delta^{2}H$, and $^{87}Sr/^{86}Sr$ provide powerful diagnostic indicators of groundwater mixing, flow-path reorganization, and deep-fluid contributions driven by seismically induced permeability enhancement. Stable isotope signatures measured after large earthquakes in Taiwan and Korea have revealed enhanced river–aquifer exchange [47], the upward intrusion of deeply circulated formation water [57], and water–rock interaction effects associated with fault rupture [54]. Dissolved gas measurements, particularly radon (^{222}Rn), thoron (^{220}Rn), methane, and helium isotopes ($^{3}He/^{4}He$), have proven highly sensitive to fracture activation and short-lived permeability increases. Large anomalies in helium isotopes following the Wenchuan earthquake, for example, indicated mantle-derived gas ascent along newly opened flow paths [50], while thoron-based monitoring in Korea demonstrated potential for detecting near-real-time fracture reactivation [58].

Multivariate and machine-learning analytical methods, including principal component analysis and SOM, have been widely used to discriminate mechanisms controlling groundwater anomalies, such as water–rock interaction, saline intrusion, and deep–shallow mixing transitions [53,43]. Time-series decomposition and spectral analysis techniques have enabled the extraction of seismic signals from seasonality, pumping, and tidal effects, allowing detection of subtle pre-seismic anomalies and quantitative evaluation of persistence in post-seismic hydrochemical responses [46]. Recent work combining gas-geochemical and microbial community observations demonstrated that microbiological signatures can serve as additional tracers of seismic-induced fracture permeability changes [58].

These monitoring and analytical strategies provide a comprehensive framework for evaluating fault-controlled hydrogeological processes and advancing predictive capability in crustal fluid-earthquake interaction research. The integration of continuous monitoring networks, multi-tracer geochemistry, and advanced analytical tools represents a critical methodological direction for future studies in seismic hydrogeology.

Research Gaps and Future Directions

Despite major advances in understanding of earthquake-induced hydrogeochemical and hydrological responses, important knowledge gaps remain regarding the mechanisms, spatial heterogeneity, and predictability of subsurface fluid behavior during seismic cycles. Most existing studies rely on post-seismic hydrochemical anomalies to infer permeability enhancement and flow-path reorganization [47,49,54], yet the causal relationships among rupture dynamics, fracture network development, and deep-fluid mobilization remain insufficiently constrained. The majority of observations are based on sparse well networks, limiting the ability to resolve the three-dimensional structure of fluid redistribution and the geometry of active flow pathways at the basin-to-fault scale. While co-seismic step responses in groundwater level have been widely observed, distinguishing between elastic pore-pressure changes and hydraulic responses driven by permeability enhancement continues to challenge interpretation, particularly in heterogeneous fractured aquifers [48].

Another limitation involves the lack of long-term, high-frequency, multi-parameter baseline datasets that capture the full progression of pre-seismic, co-seismic, and post-seismic stages. Many hydrochemical studies are opportunistic and initiated only after major events, hindering the identification of reliable precursory signals. Furthermore, although stable isotopes, noble gases, radon, and strontium isotopes have demonstrated diagnostic value for tracing deep-fluid interaction [50,57], the integration of chemical, isotopic, gaseous, and microbial tracers remains limited, and few studies link geochemical anomalies to in-situ measurements of fracture aperture changes or stress-strain evolution.

Future progress requires densely distributed, multi-sensor real-time monitoring networks combined with advanced analytical methodologies. These should include: (1) coupled hydro-mechanical-chemical modeling to evaluate feedbacks between stress, permeability, and water–rock interaction; (2) machine-learning frameworks for automated anomaly detection and signal classification; (3) joint interpretation of tracers spanning multiple residence times (e.g., $\delta^{18}O$–$\delta^{2}H$, $^{3}He/^{4}He$, ^{220}Rn, $^{87}Sr/^{86}Sr$, and microbial markers); and (4) field-scale hydraulic stimulation experiments to directly assess permeability evolution under controlled conditions. Expanding monitoring networks across active fault systems and other intraplate environments will be particularly important for improving the generalizability and predictability of earthquake-fluid coupling mechanisms. Ultimately, advancing the integration of hydrological, geochemical, geomechanical, and microbiological perspectives will be crucial for developing early-warning indicators and constraining the role of subsurface fluids in both natural and induced seismicity.

References

1. Wang CY, Manga M. Hydrologic responses to earthquakes and a general metric. Geofluids 2010;10:206-216. https://doi.org/10.1111%2Fj.1468-8123.2009.00270.x
2. Ingebritsen SE, Manga M. Hydrogeochemical precursors. Nat Geosci 2014;7:697-698. https://doi.org/10.1038/ngeo2261
3. Sano Y, Takahata N, Kagoshima T, Shibata T, Onoue T, Zhao D. Groundwater helium anomaly reflects strain change during the 2016 Kumamoto earthquake in Southwest Japan. Sci Rep 2016;6:37939. https://doi.org/10.1038/srep37939
4. Shi Z, Zhang H, Wang G. Groundwater trace elements change induced by M5.0 earthquake in Yunnan. J Hydrol 2020;581:124424. https://doi.org/10.1016/j.jhydrol.2019.124424
5. Zhang S, Shi Z, Wang G, Yan R, Zhang Z. Groundwater radon precursor anomalies identification by decision tree method. Appl Geochem 2020;121:104696. https://doi.org/10.1016/j.apgeochem.2020.104696
6. Manga M, Wang CY. 4.10 - Earthquake hydrology. Treatise Geophys 2007;4:293-320. https://doi.org/10.1016/B978-044452748-6.00074-2
7. Manga M, Beresnev I, Brodsky EE, Elkhoury JE, Elsworth D, Ingebritsen SE, et al. Changes in permeability caused by transient stresses: field observations, experiments, and mechanisms. Rev Geophys 2012;50:RG2004. https://doi.org/10.1029/2011RG000382
8. Koizumi N, Tsukuda E, Kamigaichi O, Matsumoto N, Takahashi M, Sato T. Preseismic changes in groundwater level and volumetric strain associated with earthquake swarms off the East coast of the Izu Peninsula, Japan. Geophys Res Lett 1999;26:3509-3512. https://doi.org/10.1029/1999GL005381
9. Itaba S, Koizumi N, Matsumoto N, Ohtani R. Continuous observation of groundwater and crustal deformation for forecasting Tonankai and Nankai earthquakes in Japan. Pure Appl

Geophys 2010;167:1105-1114. https://doi.org/10.1007/s00024-010-0095-z
10. Skelton A, Liljedahl-Claesson L, Wästeby N, Andrén M, Stockmann G, Sturkell E, et al. Hydrochemical changes before and after earthquakes based on long-term measurements of multiple parameters at two sites in northern Iceland: a review. J Geophys Res Solid Earth 2019;124:2702-2720. https://doi.org/10.1029/2018JB016757
11. Skelton A, Sturkell E, Mörth CM, Stockmann G, Jónsson S, Stefansson A, et al. Towards a method for forecasting earthquakes in Iceland using changes in groundwater chemistry. Commun Earth Environ 2024;5:662. https://doi.org/10.1038/s43247-024-01852-3
12. Christenson BW. Geochemistry of fluids associated with the 1995–1996 eruption of Mt. Ruapehu, New Zealand: signatures and processes in the magmatic-hydrothermal system. J Volcanol Geotherm Res 2000;97:1-30. https://doi.org/10.1016/S0377-0273(99)00167-5
13. Paudel SR, Banjara SP, Wagle A, Freund FT. Earthquake chemical precursors in groundwater: a review. J Seismol 2018;22:1293-1314. https://doi.org/10.1007/s10950-018-9739-8
14. Zhu R, Yang F, Zhou X, Tian J, Zhang Y, He M, et al. Anomaly detection using machine learning in hydrochemical data from hot springs: implications for earthquake prediction. Water Resour Res 2024;60:e2023WR034748. https://doi.org/10.1029/2023WR034748
15. Brodsky EE, Roeloffs E, Woodcock D, Gall I, Manga M. A mechanism for sustained groundwater pressure changes induced by distant earthquakes. J Geophys Res Solid Earth 2003;108:B8. https://doi.org/10.1029/2002JB002321
16. Manga M, Rowland JC. Response of Alum Rock springs to the October 30, 2007 Alum Rock earthquake and implications for the origin of increased discharge after earthquakes. Geofluids 2009;9:237-250. https://doi.org/10.1111/j.1468-8123.2009.00250.x
17. Skelton A, Andrén M, Kristmannsdóttir H, Stockmann G, Mörth CM, Sveinbjörnsdóttir Á, et al. Changes in groundwater chemistry before two consecutive earthquakes in Iceland. Nat Geosci 2014;7:752-756. https://doi.org/10.1038/ngeo2250
18. Rojstaczer S, Wolf S, Michel R. Permeability enhancement in the shallow crust as a cause of earthquake-induced hydrological changes. Nature 1995;373:237-239. https://doi.org/10.1038/373237a0
19. Wang C, Cheng LH, Chin CV, Yu SB. Coseismic hydrologic response of an alluvial fan to the 1999 Chi-Chi earthquake, Taiwan. Geology 2001;29:831-834. https://doi.org/10.1130/0091-7613(2001)029<0831:CHROAA>2.0.CO;2
20. Yamamoto S, Koike K, Yamashiki YA, Shimada J. Detecting groundwater level changes related to the 2016 Kumamoto earthquake. Sci Rep 2023;13:22916. https://doi.org/10.1038/s41598-023-50133-0
21. Christenson BW, Reyes AG, Young R, Moebis A, Sherburn S, Cole-Baker J, et al. Cyclic processes and factors leading to phreatic eruption events: insights from the 25 September 2007 eruption through Ruapehu Crater Lake, New Zealand. J Volcanol Geotherm Res 2010;191:15-32. https://doi.org/10.1016/j.jvolgeores.2010.01.008
22. Chiodini G, Cardellini C, Di Luccio F, Selva J, Frondini F, Caliro S, et al. Correlation between tectonic CO_2 Earth degassing and seismicity is revealed by a 10-year record in the Apennines, Italy. Sci Adv 2020;6:eabc2938. https://doi.org/10.1126/sciadv.abc2938
23. Zhu A, Yang Z, Liang Z, Gao L, Li R, Hou L, et al. Integrating hydrochemical and biological approaches to investigate the surface water and groundwater interactions in the hyporheic zone of the Liuxi River basin, southern China. J Hydrol 2020;583:124622. https://doi.org/10.1016/j.jhydrol.2020.124622
24. Morimura S, Zeng X, Noboru N, Hosono T. Changes to the microbial communities within

groundwater in response to a large crustal earthquake in Kumamoto, southern Japan. J Hydrol 2020;581:124341. https://doi.org/10.1016/j.jhydrol.2019.124341
25. Chemeri L, Taussi M, Cabassi J, Capecchiacci F, Randazzo A, Tassi F, et al. Groundwater and dissolved gases geochemistry in the Pesaro-Urbino province (Northern Marche, Central Italy) as a tool for seismic surveillance and sustainability. Sustainability 2024;16:5178. https://doi.org/10.3390/su16125178
26. Lee J, Kim Y, Jeong H. Effects of an earthquake on the variations of hydrogeochemistry of groundwater? A review. J Geol Soc Korea 2020;56:265-271. https://doi.org/10.14770/jgsk.2020.56.2.265
27. Zhou Z, Zhong J, Zhao J, Yan R, Tian L, Fu H. Two mechanisms of earthquake-induced hydrochemical variations in an observation well. Water 2021;13:2385. https://doi.org/10.3390/w13172385
28. Nakagawa K, Shimada J, Yu ZQ, Ide K, Berndtsson R. Effects of the Japanese 2016 Kumamoto earthquake on nitrate content in groundwater supply. Minerals 2020;11:43. https://doi.org/10.3390/min11010043
29. Chen Y, Liu J. Groundwater trace element changes were probably induced by the ML3.3 earthquake in Chaoyang district, Beijing. Front Earth Sci 2023;11:1260559. https://doi.org/10.3389/feart.2023.1260559
30. Barberio MD, Barbieri M, Billi A, Doglioni C, Petitta M. Hydrogeochemical changes before and during the 2016 Amatrice-Norcia seismic sequence (central Italy). Sci Rep 2017;7:11735. https://doi.org/10.1038/s41598-017-11990-8
31. King CY. Gas geochemistry applied to earthquake prediction: an overview. J Geophys Res Solid Earth 1986;91:12269-12281. https://doi.org/10.1029/JB091iB12p12269
32. Igarashi G, Saeki S, Takahata N, Sumikawa K, Tasaka S, Sasaki Y, et al. Ground-water radon anomaly before the Kobe earthquake in Japan. Science 1995;269:60-61. https://doi.org/10.1126/science.269.5220.60
33. Zmazek B, Todorovski L, Džeroski S, Vaupotič J, Kobal I. Application of decision trees to the analysis of soil radon data for earthquake prediction. Appl Radiat Isot 2003;58:697-706. https://doi.org/10.1016/S0969-8043(03)00094-0
34. Zmazek B, Živčić M, Todorovski L, Džeroski S, Vaupotič J, Kobal I. Radon in soil gas: how to identify anomalies caused by earthquakes. Appl Geochem 2005;20:1106-1119. https://doi.org/10.1016/j.apgeochem.2005.01.014
35. Muto J, Yasuoka Y, Miura N, Iwata D, Nagahama H, Hirano M, et al. Preseismic atmospheric radon anomaly associated with 2018 Northern Osaka earthquake. Sci Rep 2021;11:7451. https://doi.org/10.1038/s41598-021-86777-z
36. Umeda K, Ninomiya A, McCrank GF. High ^{3}He emanations from the source regions of recent large earthquakes, central Japan. Geochem Geophys Geosyst 2008;9:Q12003. https://doi.org/10.1029/2008GC002272
37. Baniya S, Paudel SR, Angove MJ, Acharya G, Wagle A, Khatri M, et al. Theoretical and earthquake-induced groundwater chemistry changes: a perspective. J Hydrol 2024;643:131917. https://doi.org/10.1016/j.jhydrol.2024.131917
38. Onda S, Sano Y, Takahata N, Kagoshima T, Miyajima T, Shibata T, et al. Groundwater oxygen isotope anomaly before the M6.6 Tottori earthquake in Southwest Japan. Sci Rep 2018;8:4800. https://doi.org/10.1038/s41598-018-23303-8
39. Liang J, Yu Y, Shi Z, Li Z, Huang Y, Song H, et al. Geothermal springs with high $\delta^{13}C_{CO2}$-DIC along the Xianshuihe fault, western Sichuan, China: a geochemical signature of enhanced deep tectonic activity. J Hydrol 2023;623:129760. https://doi.org/10.1016/

j.jhydrol.2023.129760
40. Liu Y, Liu W, Zhou X, Zhong J, Zhang M, Xu S. Carbon mobilization in response to the 2021 Mw 7.4 Maduo earthquake: constraints from carbon isotope systematics of subsurface fluids. Front Earth Sci 2023;10:1091052. https://doi.org/10.3389/feart.2022.1091052
41. Hosono T, Hartmann J, Louvat P, Amann T, Washington KE, West AJ, et al. Earthquake-induced structural deformations enhance long-term solute fluxes from active volcanic systems. Sci Rep 2018;8:14809. https://doi.org/10.1038/s41598-018-32735-1
42. Wang B, Zhou X, Zhou Y, Yan Y, Li Y, Ouyang S, et al. Hydrogeochemistry and precursory anomalies in thermal springs of Fujian (southeastern China) associated with earthquakes in the Taiwan Strait. Water 2021;13:3523. https://doi.org/10.3390/w13243523
43. Kim J, Lee J, Petitta M, Kim H, Kaown D, Park IW, et al. Groundwater system responses to the 2016 ML 5.8 Gyeongju earthquake, South Korea. J Hydrol 2019;576:150-163 https://doi.org/10.1016/j.jhydrol.2019.06.044
44. Song SR, Ku WY, Chen YL, Lin YC, Liu CM, Kuo LW, et al. Groundwater chemical anomaly before and after the Chi-Chi earthquake in Taiwan. Terr Atmos Ocean Sci 2003;14:311-320. https://doi.org/10.3319/TAO.2003.14.3.311(T)
45. Wang CY, Wang CH, Kuo CH. Temporal change in groundwater level following the 1999 (M_w = 7.5) Chi-Chi earthquake, Taiwan. Geofluids 2004;4:210-220. https://doi.org/10.1111/j.1468-8123.2004.00082.x
46. Gau HS, Chen TC, Chen JS, Liu CW. Time series decomposition of groundwater level changes in wells due to the Chi-Chi earthquake in Taiwan: a possible hydrological precursor to earthquakes. Hydrol Process 2007;21:510-524. https://doi.org/10.1002/hyp.6257
47. Wang CH, Wang CY, Kuo CH, Chen WF. Some isotopic and hydrological changes associated with the 1999 Chi-Chi earthquake, Taiwan. Island Arc 2005;14:37-54. https://doi.org/10.1111/j.1440-1738.2004.00456.x
48. Liu CY, Chia Y, Chuang PY, Chiu YC, Tseng TL. Impacts of hydrogeological characteristics on groundwater-level changes induced by earthquakes. Hydrogeol J 2018;26:451-465. https://doi.org/10.1007/s10040-017-1684-z
49. Chen Z, Du J, Zhou X, Yi L, Liu L, Xie C, et al. Hydrochemistry of the hot springs in western Sichuan province related to the Wenchuan MS 8.0 earthquake. Sci World J 2014;2014:901432. https://doi.org/10.1155/2014/901432
50. Zhou X, Wang W, Chen Z, Yi L, Liu L, Xie C, et al. Hot spring gas geochemistry in western Sichuan province, China after the Wenchuan Ms 8.0 earthquake. Terr Atmos Ocean Sci 2015;26:361. https://doi.org/10.3319/TAO.2015.01.05.01(TT)
51. Chen Z, Zhou X, Du J, Xie C, Liu L, Li Y, et al. Hydrochemical characteristics of hot spring waters in the Kangding district related to the Lushan M_S = 7.0 earthquake in Sichuan, China. Nat Hazards Earth Syst Sci 2015;15:1149-1156. https://doi.org/10.5194/nhess-15-1149-2015
52. Hosono T, Yamada C, Manga M, Wang CY, Tanimizu M. Stable isotopes show that earthquakes enhance permeability and release water from mountains. Nat Commun 2020;11:2776. https://doi.org/10.1038/s41467-020-16604-y
53. Kaown D, Koh DC, Kim H, Koh HJ, Kim J, Lee S, et al. Evaluating the responses of alluvial and bedrock aquifers to earthquakes (M_L5.1 and M_L5.8) using hydrological and environmental tracer data. Hydrogeol J 2019;27:2011-2025. https://doi.org/10.1007/s10040-019-01966-5
54. Kim J, Joun WT, Lee S, Kaown D, Lee KK. Hydrogeochemical evidence of earthquake-induced anomalies in response to the 2017 MW 5.5 Pohang earthquake in Korea. Geochem Geophys Geosyst 2020;21:e2020GC009532. https://doi.org/10.1029/2020GC009532

55. Lee SH, Lee JM, Moon SH, Ha K, Kim Y, Jeong DB, et al. Seismically induced changes in groundwater levels and temperatures following the M_L5.8 (M_L5.1) Gyeongju earthquake in South Korea. Hydrogeol J 2021;29:1679-1689. https://doi.org/10.1007/s10040-021-02328-w
56. Lee JM, Woo NC, Koh DC, Kim KY, Ko KS. Assessing aquifer responses to earthquakes using temporal variations in groundwater monitoring data in alluvial and sedimentary bedrock aquifers. Geomat Nat Hazards Risk 2020;11:742-765. https://doi.org/10.1080/19475705.2020.1751310
57. Kaown D, Lee KK, Kim J, Woo JU, Lee S, Park IW, et al. Earthquakes and very deep groundwater perturbation mutually induced. Sci Rep 2021;11:13632. https://doi.org/10.1038/s41598-021-92937-y
58. Kim J, Kim H, Kaown D, Lee KK. Thoron, radon and microbial community as supportive indicators of seismic activity in groundwater. Sci Rep 2024;14:25955. https://doi.org/10.1038/s41598-024-77011-7
59. Tsunomori F, Shimodate T, Ide T, Tanaka H. Radon concentration distributions in shallow and deep groundwater around the Tachikawa fault zone. J Environ Radioact 2017;172:106-112. https://doi.org/10.1016/j.jenvrad.2017.03.009
60. Orihara Y, Kamogawa M, Nagao T. Preseismic changes of the level and temperature of confined groundwater related to the 2011 Tohoku earthquake. Sci Rep 2014;4:6907. https://doi.org/10.1038/srep06907
61. Roy K, Sasada K, Kohno E. Salinity status of the 2011 Tohoku-oki tsunami affected agricultural lands in Northeast Japan. Int Soil Water Conserv Res 2014;2:40-50. https://doi.org/10.1016/S2095-6339(15)30005-8
62. Westaway R, Burnside NM, Banks D. Hydrochemistry of produced water from the Pohang EGS project site, Korea: implications for water-rock reactions and associated changes to the state of stress accompanying hydraulic fracturing of granite. In: Proceedings of the World Geothermal Congress 2021; 2021 Oct 24-27; Reykjavik, Iceland.